24. J. J. Warren, T. A. Tronic, J. M. Mayer, *Chem. Rev.* **110**, 6961 (2010).
25. M. K. Mahanthappa, K.-W. Huang, A. P. Cole, R. M. Waymouth, *Chem. Commun. (Camb.)* **2002**, 502 (2002).
26. M. K. Mahanthappa, A. P. Cole, R. M. Waymouth, *Organometallics* **23**, 836 (2004).
27. K. Schröder *et al.*, *Organometallics* **27**, 1859 (2008).
28. J. M. Mayer, *Acc. Chem. Res.* **44**, 36 (2011).
29. J. Jin, M. Newcomb, *J. Org. Chem.* **73**, 7901 (2008).
30. S. Morrison, *Electrochemistry at Semiconductor and Oxidized Metal Electrodes* (Plenum, New York, 1980).
31. B. Enright, G. Redmond, D. Fitzmaurice, *J. Phys. Chem.* **98**, 6195 (1994).
32. F. Marken, A. S. Bhambra, D.-H. Kim, R. J. Mortimer, S. J. Stott, *Electrochem. Commun.* **6**, 1153 (2004).
33. M. Zukalova, M. Kalbáč, L. Kavan, I. Exnar, M. Graetzel, *Chem. Mater.* **17**, 1248 (2005).
34. A. Minguzzi, F.-R. F. Fan, A. Vertova, S. Rondinini, A. J. Bard, *Chem. Sci.* **3**, 217 (2012).
35. Y. Ren, L. J. Hardwick, P. G. Bruce, *Angew. Chem. Int. Ed.* **49**, 2570 (2010).
36. C. Venkataraman, A. V. Soudackov, S. Hammes-Schiffer, *J. Phys. Chem. C* **114**, 487 (2010).
37. H. Petek, J. Zhao, *Chem. Rev.* **110**, 7082 (2010).
38. C. Costentin, *Chem. Rev.* **108**, 2145 (2008).

Acknowledgments: Materials and methods and additional figures are presented in the supplementary materials on *Science* Online. We are grateful for financial support from the University of Washington, the American Chemical Society Petroleum Research Fund (51178-ND3), and the U.S. NSF (CHE-1151726). This research is also supported in part by the Department of Energy Office of Science Graduate Fellowship Program, made possible in part by the American Recovery and Reinvestment Act of 2009, administered by Oak Ridge Institute for Science and Education–Oak Ridge Associated Universities under contract no. DE-AC05-06OR23100, and in part by the NSF Center for Enabling New Technologies through Catalysis. We especially thank D. Gamelin, members of the Gamelin laboratory, and L. Maibaum for very valuable discussions.

Supplementary Materials

www.sciencemag.org/cgi/content/full/336/6086/1298/DC1
Materials and Methods
Supplementary Text
Figs. S1 to S14
Table S1
References (*39*–*54*)

7 February 2012; accepted 10 April 2012
10.1126/science.1220234

Interglacial Hydroclimate in the Tropical West Pacific Through the Late Pleistocene

A. N. Meckler,[1,2*] M. O. Clarkson,[3] K. M. Cobb,[4] H. Sodemann,[5] J. F. Adkins[1]

Records of atmospheric carbon dioxide concentration (P_{CO_2}) and Antarctic temperature have revealed an intriguing change in the magnitude of interglacial warmth and P_{CO_2} at around 430,000 years ago (430 ka), but the global climate repercussions of this change remain elusive. Here, we present a stalagmite-based reconstruction of tropical West Pacific hydroclimate from 570 to 210 ka. The results suggest similar regional precipitation amounts across the four interglacials contained in the record, implying that tropical hydroclimate was insensitive to interglacial differences in P_{CO_2} and high-latitude temperature. In contrast, during glacial terminations, drying in the tropical West Pacific accompanied cooling events in northern high latitudes. Therefore, the tropical convective heat engine can either stabilize or amplify global climate change, depending on the nature of the climate forcing.

The study of past interglacial climates provides valuable insight into natural climate variability under conditions roughly similar to those of the present day, but with differences in atmospheric carbon dioxide concentration (P_{CO_2}) (*1*) and astronomic forcing. Especially intriguing is a step-like increase in interglacial Antarctic temperature (*2*), global ice melting (*3*), and P_{CO_2} (*4*, *5*) that took place at roughly 430,000 years ago (430 ka) and is referred to as the Mid-Brunhes Event (MBE). To understand the underlying cause of this shift toward warmer interglacials, it is crucial to establish the global signature of interglacial climates during that time, but sufficiently long records, especially from low latitudes and terrestrial archives, are sparse. Because P_{CO_2} and ice cover affect the planet's radiative balance, a global change in interglacial climate at the MBE might be expected. Although many marine sea surface temperature (SST) reconstructions from around the globe show qualitatively similar changes to those observed in Antarctica (*6*), the few available lower-latitude SST reconstructions (*7*–*9*) from this time period do not show the same consistent increase in post-MBE interglacial temperatures. Given that many models simulate strong dynamical links between high-latitude and tropical climate [e.g., (*10*)], more tropical records are required to test and improve our understanding of low-latitude climate sensitivity to a range of different forcing factors.

Here, we present stalagmite records from northern Borneo (4°N, 115°E; fig. S1) that span several glacial-to-interglacial cycles and include the MBE. We reconstruct Warm Pool hydroclimate from the oxygen isotope ($\delta^{18}O$) variability recorded in three stalagmites with overlapping growth periods. Borneo lies in the West Pacific Warm Pool, which is an important heat and moisture source for higher latitudes (*11*). Although there is little seasonality in modern rainfall amount at our site, the isotopic composition of precipitation varies seasonally by up to 2 to 3‰ (*12*), with the most enriched $\delta^{18}O$ values occurring in February and March, when the intertropical convergence zone (ITCZ) is furthest south of our site. However, on interannual time scales, the El Niño–Southern Oscillation (ENSO) phenomenon dominates both precipitation amount and $\delta^{18}O$, with El Niño events resulting in large-scale drying and rainfall $\delta^{18}O$ that is roughly 5 to 6‰ higher than average (*12*). Two recent studies of water isotopes in the same area conclude that regional (much more than local) rainfall amount is the main driver for rainfall $\delta^{18}O$ variability on intraseasonal and longer time scales today (*13*) and during modeled millennial-scale events in the past (*14*).

We analyzed stalagmites from three different caves in Gunung Mulu and Gunung Buda National Parks, each about 5 to 10 km apart. The stalagmites were dated by ^{238}U-^{234}U-^{230}Th measurements (*15*) and cover the time period from 570 (±20) ka to 210 (±10) ka [from marine isotope stage (MIS) 13 to the beginning of MIS7], with some gaps due to hiatuses. Sample GC08 covers the whole time period, whereas samples Squeeze1 and WR5 yield shorter records that overlap GC08. In comparison to other cave systems, dating of these stalagmites is challenging due to their unusually low $^{234}U/^{238}U$ ratios and/or low U concentrations (fig. S4 and tables S1 to S3). The old age of the samples exacerbates these dating issues. Furthermore, there is evidence that slight open-system exchange of U has affected sample GC08, requiring us to model the ages in this stalagmite by assuming a constant initial $^{234}U/^{238}U$ ratio (*15*). Varying detrital ^{230}Th contamination cannot explain the age reversals in this stalagmite, owing to the short half-life of ^{230}Th compared to the age of our samples (*15*). The error assigned to the assumed constant initial $^{234}U/^{238}U$ ratio leads to increased age uncertainty in the GC08 chronology, with individual age errors ranging from ±9200 to ±13,500 years (2σ; table S1), limiting our ability to compare the millennial-scale timing of climate change in Borneo with other records. The age constraints are sufficient, however, to identify each interglacial stage, which is the main focus of this study. In sample WR5, open-system alteration might also have occurred but cannot be corrected for (*15*). The $\delta^{18}O$ record from this stalagmite therefore

[1]Geological and Planetary Science Department, California Institute of Technology, Pasadena, CA, USA. [2]Geological Institute, ETH Zurich, Switzerland. [3]School of Geosciences, University of Edinburgh, Edinburgh EH9 3JW, UK. [4]School of Earth and Atmospheric Sciences, Georgia Institute of Technology, Atlanta, GA 30332, USA. [5]Institute for Atmosphere and Climate, ETH Zurich, Switzerland.

*To whom correspondence should be addressed. E-mail: nele.meckler@erdw.ethz.ch

only serves as a check on the overall structure of the GC08 $\delta^{18}O$ record. In contrast, sample Squeeze1 yielded a reliable age model without age reversals and can be used to confirm that the stalagmite $\delta^{18}O$ records are not affected by the process(es) that altered the U isotopic composition in GC08 (and potentially WR5).

Samples for oxygen isotope analysis (*15*) were drilled along the stalagmite growth axes at 1-mm increments, which on average corresponds to 75 years in Squeeze1, 650 years in GC08, and 1000 years in WR5. Equilibrium calcite precipitation with respect to $\delta^{18}O$ is supported by several lines of evidence (*15*) (fig. S2), most importantly by the good reproducibility (within age uncertainty) of the $\delta^{18}O$ signal in the three stalagmites from different caves (Figs. 1 and 2 and fig. S3). Hence, the variations in carbonate $\delta^{18}O$ are expected to faithfully record changes in the $\delta^{18}O$ of drip water (modulated by any changes in the equilibrium carbonate-water fractionation due to changes in cave temperature). The reproducibility of the carbon isotope ($\delta^{13}C$) records from Borneo is generally much poorer (fig. S3), suggesting that this proxy is governed by cave-specific factors (*16*), with climate exerting a lesser influence.

The stalagmite $\delta^{18}O$ time series reveal large variations with maximum peak-to-peak differences of 3.0 to 4.3‰. Both the peak-to-peak differences and the absolute values of $\delta^{18}O$ are similar to those of the Borneo stalagmite record spanning the last glacial termination (*17*) (Fig. 1, yellow-orange lines). During the last deglaciation, the highest $\delta^{18}O$ values were observed just after the Last Glacial Maximum, during the time of Heinrich Event 1, and were interpreted as reflecting strong regional drying (*17*). Although their exact timing and duration are not resolvable by our age model, we interpret the pronounced $\delta^{18}O$ maxima (–5.6 to –6.6‰) in the longer record likewise, as deglacial drying phases that occurred after glacial maxima. Apart from these distinct deglacial periods, maximum glacial $\delta^{18}O$ values are –7.2 to –7.3‰ (table S4), similar to values for the Last Glacial Maximum. Interglacial periods are characterized by minimum $\delta^{18}O$ values of –9.3 to –9.5‰, comparable to values for actively growing stalagmites from northern Borneo caves.

Glacial-to-interglacial (G-IG) changes of 2.0 to 2.2‰ in stalagmite $\delta^{18}O$ represent a combination of changes in temperature and the $\delta^{18}O$ of precipitation (table S4). G-IG temperature-change estimates in the surrounding warm pool are 1.0° to 4.5°C during the same time interval (*7*, *9*) (Fig. 2E), which would only account for variations in stalagmite $\delta^{18}O$ of 0.2 to 0.9‰, if cave temperature change was the same. Therefore, most of the G-IG changes in stalagmite $\delta^{18}O$ must be due to changes in the $\delta^{18}O$ of precipitation, reflecting changes in source water $\delta^{18}O$, atmospheric moisture transport pathway, or regional precipitation amount. Reconstructed glacial enrichment in source water $\delta^{18}O$ was +0.6 to +1.3‰ (*7*, *9*) and is poorly constrained (fig. S9 and table S4). On glacial-interglacial time scales, moisture transport to Borneo was likely influenced by the varying exposure of the adjacent Sunda Shelf (fig. S1), but the effect on the $\delta^{18}O$ of rainfall is difficult to constrain. The probably increased length of moisture transport pathways, especially over land, could have led to isotopically more depleted rainfall during glacial maxima, counteracting temperature and source water $\delta^{18}O$ changes. Although the magnitude therefore remains uncertain, we interpret the stalagmite $\delta^{18}O$ record as reflecting changes in regional hydrology, with drier glacial periods (higher $\delta^{18}O$) compared to interglacials (lower $\delta^{18}O$).

The overall structure of the Borneo record suggests a strong precession influence (Fig. 2), similar to that in records of the East Asian and Australian-Asian summer monsoons (*18*, *19*). The phasing of the Borneo stalagmite $\delta^{18}O$ record with respect to precession cannot be constrained with confidence, given the age constraints. Of particular note, the new records clearly reflect a diminished precessional cyclicity between 460 and 360 ka, when precessional forcing was weak. The 100,000-year (100 ky) glacial-interglacial cycle is also apparent in Borneo, most prominently in the pronounced deglacial $\delta^{18}O$ maxima. However, the dominance of the precession signal indicates that regional changes in the seasonal distribution of insolation have a large influence on tropical West Pacific hydroclimate, compared to the effects of high-latitude climate change, which is characterized by strong 100-ky "sawtooth" variability (Fig. 2D).

In contrast to records of P_{CO_2} and high-latitude climate, the Borneo stalagmite $\delta^{18}O$ record shows no change in the magnitude of interglacial values across the MBE. The average peak interglacial $\delta^{18}O$ value for MIS13 (–9.31 ± 0.12‰, 1 SD, $N = 11$) is indistinguishable from those of MIS11 (–9.33 ± 0.25‰), MIS9 (–9.54 ± 0.11‰), and MIS7 (–9.43 ± 0.12‰). This finding is robust with regard to age uncertainties and will be discussed in more detail below. The duration of MIS11 in the Borneo stalagmite $\delta^{18}O$ records seems much longer than in other climate records (Fig. 2), although dating errors are large during this interval. Within MIS11 and MIS9, $\delta^{18}O$ varies by 0.6 to 1.2‰ (range of differences between adjacent maxima and minima), similar to the change in $\delta^{18}O$ over the course of the Holocene (*17*). Although our age model does not permit assessment of the length of such suborbital features, both of the stalagmite $\delta^{18}O$ records that span MIS11 reveal at least six distinct $\delta^{18}O$ excursions, indicating that substantial climate variability occurred in the tropical West Pacific during past interglacials.

The large, steep increases in $\delta^{18}O$ during terminations cannot be explained by changes in temperature or source water composition and imply substantial hydrological changes, possibly associated with profound drought. A drastic circulation change could also cause elevated $\delta^{18}O$ of precipitation—for example, through a more

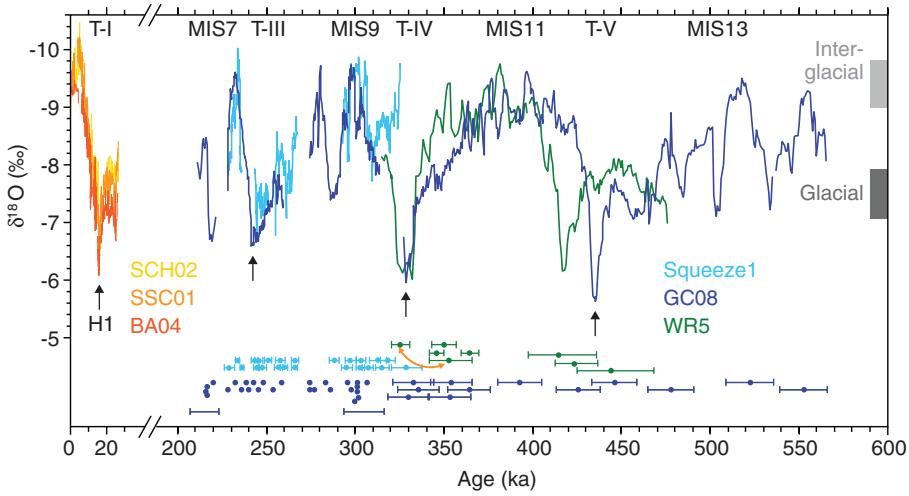

Fig. 1. Borneo stalagmite $\delta^{18}O$ records. Data from this study are from samples GC08 (dark blue), Squeeze1 (light blue), and WR5 (green), with age markers and 2σ error bars shown below. Also plotted is the published record for the last glacial termination from the same location (*17*) (yellow-orange lines). Interglacial marine isotope stages (MIS) and glacial terminations (T-) are indicated at the top, and H1 is Heinrich event 1. Light and dark gray bars on the right show range of interglacial and glacial values, respectively, and black arrows highlight $\delta^{18}O$ maxima interpreted as deglacial drying phases. The age model of GC08 is based on the assumption of constant initial $\delta^{234}U$, to correct for open-system behavior (*15*). For GC08, the age error bars therefore include the assigned error of the initial $\delta^{234}U$ of ±12‰, in addition to analytical errors. In the younger part of the GC08 record, the range of age errors is indicated by smallest and largest error bar below age markers. The orange double-arrow highlights a large age reversal in WR5 (compare to fig. S5). Within age uncertainty, the $\delta^{18}O$ signal replicates well among the three different caves. Both trends and absolute values are similar to the record for T-I.

local vapor source or a strong dominance of northern trajectories, which today bring the most enriched rainfall (*12*). One possible scenario is that the ITCZ was shifted sufficiently south that it remained south of northern Borneo during most of the year, affecting both water vapor transport and regional rainfall amount. The combination of early Southern Hemisphere warming and millennial-scale cooling in the Northern Hemisphere, accompanied by changes in ocean circulation, could have triggered such conditions (*20*). This possibility is consistent with the Weak Monsoon Intervals observed in China during the last four terminations (*18*) (Fig. 2F). It is interesting to note that the magnitude of the stalagmite $\delta^{18}O$ maxima that occur during glacial terminations decreases progressively from Termination V to Termination III, similar to the observed trend in glacial ice volume (*3*) (Fig. 2D) and other marine records (*21*), but unlike Antarctic temperature and global P_{CO_2}. This trend cannot be explained by changes in source water $\delta^{18}O$ (table S4). Although it is possible that we missed the most positive $\delta^{18}O$ excursions during Terminations IV and III due to hiatuses, the similarity of the trend in stalagmite $\delta^{18}O$ maxima to the trend in benthic $\delta^{18}O$, a proxy for glacial ice volume, is pronounced. If it holds true, this observation lends support to studies linking the size and instability of northern hemispheric ice sheets to the severity of deglacial Heinrich events and associated displacements of ITCZ and mid-latitude wind systems (*20*, *21*).

Our data show that in northern Borneo hydroclimate varied substantially within interglacials, but did not change across the MBE, suggesting that the step change in high-latitude interglacial climate did not extend into the deep tropics. This notion is supported by the small change in interglacial temperature in tropical SST records (*8*) and the absence of the MBE in some terrestrial records from lower mid-latitudes (*22*–*24*). That the post-MBE increase in interglacial P_{CO_2} did not seem to affect low-latitude climate may be an earlier manifestation of the "polar amplification effect" (*25*), whereby high-latitude albedo-related feedbacks involving changes in sea ice and/or snow cover translate to a larger sensitivity of high-latitude climate to changes in greenhouse gas forcing (*26*). Additionally, the geographic pattern of climate responses might have been modulated by variations in Earth's orbital configuration, as proposed by a recent modeling study (*27*) suggesting that insolation changes counteracted the MBE change in P_{CO_2} in the Northern Hemisphere. However, existing records from northern mid- to high latitudes are equivocal (*28*, *29*).

With small changes in interglacial temperature suggested by tropical SST records, the latitudinal temperature gradient decreased in post-MBE interglacials, but apparently with no discernible effect on tropical West Pacific hydrology. Instead, overhead insolation remained the dominant forcing factor during interglacials, irrespective of changing P_{CO_2} and latitudinal temperature gradients, providing an important target for climate model simulations. As the region is an important heat and moisture source for the global climate system (*11*), the lack of response to the high-latitude MBE change could potentially have been transferred to the mid-latitudes. The strong drying observed during terminations, by contrast, may imply less moisture and latent heat export, constituting a potential positive-feedback mechanism during the millennial-scale high-latitude cooling events. This difference in response suggests that with regard to high-latitude climate forcing, tropical West Pacific climate may be more sensitive to transient and/or rapid changes in high-latitude climate and ocean circulation than to differences in steady state.

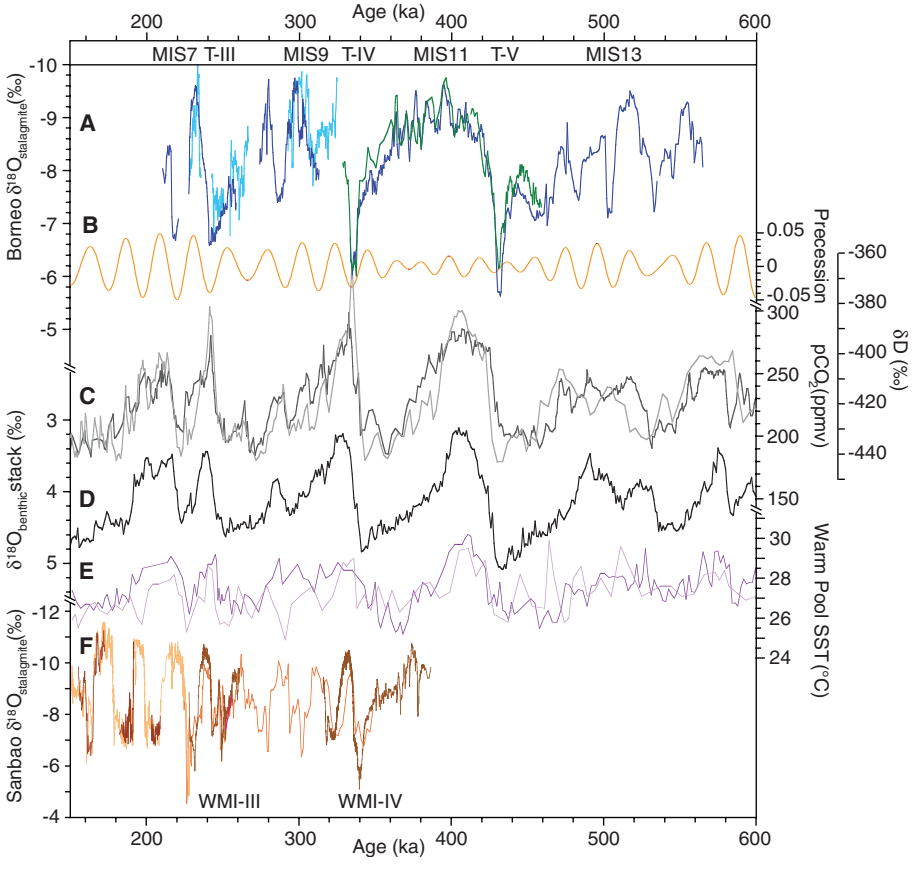

Fig. 2. Comparison of the Borneo stalagmite $\delta^{18}O$ record with other climate records. (**A**) Stalagmite record with adjusted age models for GC08 and WR5 (see below); (**B**) the precession parameter (*30*); (**C**) atmospheric P_{CO_2} (dark gray) (*4*, *5*) and Antarctic δD, a proxy for temperature (light gray) (2); (**D**) global stack of benthic $\delta^{18}O$ (*3*) as a proxy for global ice volume; (**E**) West Pacific Warm Pool SST reconstructed from Mg/Ca in foraminifera from the Ontong Java Plateau (dark purple) (*7*) and off Indonesia (light purple) (9); (**F**) East Asian Monsoon record from Sanbao/Linzhu caves (*18*). Indicated on top are interglacial marine isotope stages (MIS) and glacial terminations (T-). The age model of GC08 has been slightly modified around T-IV (+5 ky, within 1σ age errors) to better align the $\delta^{18}O$ peak to the decrease in benthic $\delta^{18}O$. The WR5 record, which has the largest age uncertainty of our three records, has been tuned to the GC08 record to facilitate comparison (*15*). Unlike P_{CO_2}, ice volume, and Antarctic temperature, the climate in Borneo does not show a change in the level of peak interglacial values from MIS13 to MIS11. Maximum $\delta^{18}O$ values during terminations resemble similar events in China (weak monsoon intervals, WMI), with the signal standing out more in the Borneo record. Note the apparent trend in magnitude of these deglacial signals in Borneo from T-V to T-III, which resembles the trend in ice volume during preceding glacial periods.

References and Notes

1. P. C. Tzedakis *et al.*, *Nat. Geosci.* **2**, 751 (2009).
2. J. Jouzel *et al.*, *Science* **317**, 793 (2007).
3. L. E. Lisiecki, M. E. Raymo, *Paleoceanography* **20**, PA1003 (2005).
4. D. Lüthi *et al.*, *Nature* **453**, 379 (2008).
5. U. Siegenthaler *et al.*, *Science* **310**, 1313 (2005).
6. N. Lang, E. W. Wolff, *Clim. Past* **7**, 361 (2011).
7. M. Medina-Elizalde, D. W. Lea, *Science* **310**, 1009 (2005).
8. T. D. Herbert, L. C. Peterson, K. T. Lawrence, Z. H. Liu, *Science* **328**, 1530 (2010).
9. T. de Garidel-Thoron, Y. Rosenthal, F. Bassinot, L. Beaufort, *Nature* **433**, 294 (2005).
10. J. C. H. Chiang, C. M. Bitz, *Clim. Dyn.* **25**, 477 (2005).
11. P. Knippertz, H. Wernli, *J. Clim.* **23**, 987 (2010).
12. K. M. Cobb, J. F. Adkins, J. W. Partin, B. Clark, *Earth Planet. Sci. Lett.* **263**, 207 (2007).
13. N. Kurita, K. Ichiyanagi, J. Matsumoto, M. D. Yamanaka, T. Ohata, *J. Geochem. Explor.* **102**, 113 (2009).
14. S. C. Lewis, A. N. LeGrande, M. Kelley, G. A. Schmidt, *Clim Past* **6**, 325 (2010).

15. Materials and methods are available as supplementary materials on *Science* Online.
16. I. J. Fairchild *et al.*; e.i.M.F., *Earth Sci. Rev.* **75**, 105 (2006).
17. J. W. Partin, K. M. Cobb, J. F. Adkins, B. Clark, D. P. Fernandez, *Nature* **449**, 452 (2007).
18. H. Cheng *et al.*, *Science* **326**, 248 (2009).
19. K. Tachikawa *et al.*, *Quat. Sci. Rev.* **30**, 3716 (2011).
20. G. H. Denton *et al.*, *Science* **328**, 1652 (2010).
21. E. Bard, R. E. M. Rickaby, *Nature* **460**, 380 (2009).
22. P. C. Tzedakis, H. Hooghiemstra, H. Pälike, *Quat. Sci. Rev.* **25**, 3416 (2006).
23. P. J. Fawcett *et al.*, *Nature* **470**, 518 (2011).
24. Q. Z. Yin, Z. T. Guo, *Clim. Past* **4**, 29 (2008).
25. S. Manabe, R. J. Stouffer, *J. Geophys. Res.* **85**, 5529 (1980).
26. M. M. Holland, C. M. Bitz, *Clim. Dyn.* **21**, 221 (2003).
27. Q. Z. Yin, A. Berger, *Nat. Geosci.* **3**, 243 (2010).
28. K. T. Lawrence, T. D. Herbert, C. M. Brown, M. E. Raymo, A. M. Haywood, *Paleoceanography* **24**, PA2218 (2009).
29. I. Candy *et al.*, *Earth Sci. Rev.* **103**, 183 (2010).
30. J. Laskar *et al.*, *Astron. Astrophys.* **428**, 261 (2004).

Acknowledgments: We thank B. Clark, S. Lejau, and J. Malang of Mulu National Park, as well as J. Partin for assistance in the field. A. Tuen (Universiti Malaysia Sarawak) greatly facilitated fieldwork in Sarawak. N. Sharma and K. Stewart are acknowledged for assistance with stable isotope measurements. D. Lund, A. Subhas, and D. Fernandez are thanked for assistance and advice with U-Th dating. J. Eiler provided access to his facilities at the California Institute of Technology. Support for this work was provided by the Swiss National Science Foundation (SNF) and the German Research Foundation (DFG) through postdoctoral fellowships to A.N.M.; by the US NSF through grants ATM-0318445 and ATM-0903099 to J.F.A, as well as ATM-0645291 to K.M.C.; and by an Edinburgh University Principal's Career Development Ph.D. Scholarship to M.O.C.

Supplementary Materials

www.sciencemag.org/cgi/content/full/science.1218340/DC1
Materials and Methods
Figs. S1 to S9
Tables S1 to S4
References (*31*–*39*)

22 December 2011; accepted 19 April 2012
Published online 3 May 2012;
10.1126/science.1218340

Global Honey Bee Viral Landscape Altered by a Parasitic Mite

Stephen J. Martin,[1]* Andrea C. Highfield,[2] Laura Brettell,[1] Ethel M. Villalobos,[3] Giles E. Budge,[4] Michelle Powell,[4] Scott Nikaido,[3] Declan C. Schroeder[2]*

Emerging diseases are among the greatest threats to honey bees. Unfortunately, where and when an emerging disease will appear are almost impossible to predict. The arrival of the parasitic *Varroa* mite into the Hawaiian honey bee population allowed us to investigate changes in the prevalence, load, and strain diversity of honey bee viruses. The mite increased the prevalence of a single viral species, deformed wing virus (DWV), from ~10 to 100% within honey bee populations, which was accompanied by a millionfold increase in viral titer and a massive reduction in DWV diversity, leading to the predominance of a single DWV strain. Therefore, the global spread of *Varroa* has selected DWV variants that have emerged to allow it to become one of the most widely distributed and contagious insect viruses on the planet.

The emergence of infectious diseases is driven largely by socioeconomic, environmental, and ecological factors (*1*), and these diseases have significant effects on biodiversity, agricultural biosecurity, global economies, and human health (*2*, *3*). The honey bee is one of the most economically important insects, providing crop pollination services and valuable hive products (*4*). During the past 50 years, the global spread of the ectoparasitic mite *Varroa destructor* has resulted in the death of millions of honey bee (*Apis mellifera*) colonies (*5*). There is general consensus that the mites' association with a range of honey bee RNA viruses is a contributing factor in the global collapse of honey bee colonies (*5*–*10*), because the spread of mites has facilitated the spread of viruses (*11*, *12*) by acting as a viral reservoir and incubator (*13*). In addition, the mites' feeding behavior allows virus to be transmitted directly into the bees' hemolymph, thus bypassing conventional, established oral and sexual routes of transmission. In particular, deformed wing virus (DWV) has been associated with the collapse of *Varroa*-infested honey bee colonies (*5*, *8*, *14*–*16*), because it is ubiquitous in areas where *Varroa* is well established (*6*, *9*, *17*, *18*). The rapid global spread of *Varroa* means that very little is known about the natural prevalence, viral load, and strain diversity of honey bee viruses before the *Varroa* invasion (*15*). Such data are important, because most honey bee viral infections were considered harmless before the spread of *Varroa* (*9*). Large-scale loss of honey bee colonies has been associated with viruses vectored by *Varroa* (*5*). The recent arrival and subsequent spread of *Varroa* across parts of the Hawaiian archipelago has provided an opportunity to study the initial phase of the evolution of the honey bee–*Varroa*–DWV association. So far, colony collapse disorder (CCD) (*6*) has not been reported in Hawaii (*19*), but all of the associated pests and pathogens are present.

European honey bees (*Apis mellifera* L.) were first introduced to Hawaii from California in 1857. They were largely managed, but feral populations were soon established on every major island in the archipelago (*20*). Hawaii remained *Varroa*-free until August 2007, when the mite was discovered throughout Oahu Island. A subsequent survey by S. Nikaido and E. Villalobos during 2007–2008 recorded the collapse of 274 of 419 untreated colonies belonging to beekeepers. The disappearance of feral colonies from urban areas on Oahu was also noticed by beekeepers and pest control officers. Despite quarantine measures, the mite spread to Hilo on the Big Island in January 2009, where it survived an eradication attempt and by November 2009 had spread throughout the southern region of the island (Fig. 1). By November 2010, *Varroa* occurred throughout the Big Island. However, the islands of Kauai and Maui remained mite-free, and no unusual colony losses or disease problems have been reported there (*19*). The aim of this study was to investigate the influence that *Varroa* has in the spread of honey bee viruses during the initial

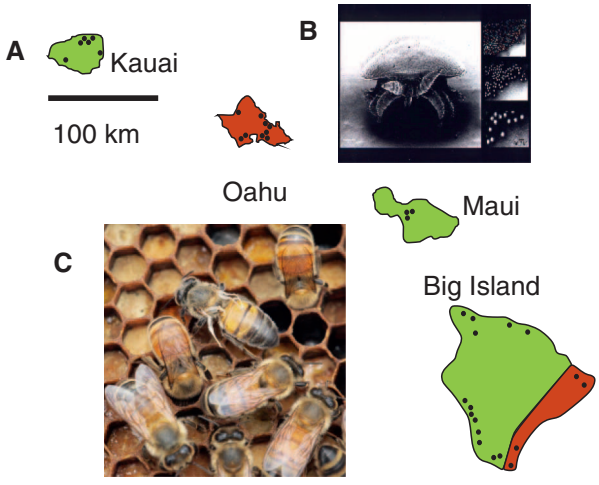

Fig. 1. (**A**) The four main Hawaiian Islands, showing the distribution of *Varroa* during 2009. Green and brown indicate *Varroa*-free and *Varroa* infested areas respectively. Dots indicate the location of each study apiary. By November 2010, *Varroa* was present throughout the Big Island. The co-occurrence of the *Varroa* mite (**B**) and DWV can result in overt symptoms of (**C**) deformed wings in honey bees, although many nondeformed bees also carry high DWV loads.

[1]Department of Animal and Plant Sciences, University of Sheffield, Sheffield S10 2TN, UK. [2]The Marine Biological Association of the United Kingdom, Citadel Hill, Plymouth PL1 2PB, UK. [3]Department of Plant and Environmental Protection Sciences, University of Hawaii at Manoa, Hawaii, USA. [4]The Food and Environment Research Agency, Sand Hutton, York YO41 1LZ, UK.

*To whom correspondence should be addressed. E-mail: s.j.martin@sheffield.ac.uk (S.J.M.); dsch@mba.ac.uk (D.C.S.)